

Cooperative Organization of Inorganic-Surfactant and Biomimetic Assemblies

A. Firouzi, D. Kumar, L. M. Bull, T. Besier, P. Sieger, Q. Huo, S. A. Walker, J. A. Zasadzinski, C. Glinka, J. Nicol, D. Margolese, G. D. Stucky, B. F. Chmelka*

A model that makes use of the cooperative organization of inorganic and organic molecular species into three dimensionally structured arrays is generalized for the synthesis of nanocomposite materials. In this model, the properties and structure of a system are determined by dynamic interplay among ion-pair inorganic and organic species, so that different phases can be readily obtained through small variations of controllable synthesis parameters, including mixture composition and temperature. Nucleation, growth, and phase transitions may be directed by the charge density, coordination, and steric requirements of the inorganic and organic species at the interface and not necessarily by a preformed structure. A specific example is presented in which organic molecules in the presence of multiply charged silicate oligomers self-assemble into silicotropic liquid crystals. The organization of these silicate-surfactant mesophases is investigated with and without interfacial silicate condensation to separate the effects of self-assembly from the kinetics of silicate polymerization.

Currently, a central tenet of biomineralization models (1) is that nucleation, growth, and the final morphology of the inorganic species are determined by preorganized assemblies of organic molecules. "Biomimetic" syntheses and modeling of biomineralization have relied on this paradigm for experimental design, which begins with a preorganized organic surface that directs the subsequent nucleation and growth of the inorganic species. Implicit in this view is that the geometry of the organic template is preserved as nucleation and growth of a biomineral or an inorganic-organic composite proceed. Consequently, the morphological or phase changes of phospholipid and surfactant assemblies that generally accompany changes in temperature or ion concentration have presented a serious complication to this model of biomimetic synthesis. Biomimetic synthesis strategies have accordingly focused on the use of known stable organic arrays or the stabilization of the organic groups through, for example, covalent attachment to a substrate or crosslinking. Recent developments in this area include the use of hollow, submicrometer-diameter silica cylinders obtained by depositing silica onto phospholipid tubules (2), bulk inorganic iron oxide deposited on charged biolipid substrates (3), and ceramic thin-film processing by deposition of bulk

inorganic phases on surfaces functionalized with ionic organic surfactants (4).

In this report we describe an alternative procedure for inorganic-surfactant and biomimetic self-assembly. This view is based on cooperative organization and is consistent with the generation of one-, two-, or three-dimensional periodic arrays of inorganic-organic assemblies formed from surfactant molecules and inorganic ions (5-11). In all cases, the ultimate structure and symmetry are determined by dynamic and often subtle interactions among the organic and inorganic species according to equilibrium thermodynamics. Organic arrays that have long-range preorganized order are not required as substrates for nucleation of the inorganic phase. Moreover, a micellar assembly of organic molecules will often rearrange upon addition of inorganic species to form new and often unexpected morphologies. The structure and phase behavior of the composite inorganic-organic assembly are particularly dependent on the nature of the inorganic species and its electrostatic and steric interactions with the organic species. Temperature, ionic strength, pH, and concentration control the direction and nature of the growth of the organized array.

In part because of the relatively low concentration of organic species often present in biomimetic and biomineralization processes [0.01 to 5.0% of the total mass (12)], the role of the organic matrix has been elusive and difficult to characterize. Thus, we investigated inorganic-organic mesophase syntheses with low organic concentrations. As indicated in the synthesis-space diagram for a silicate-surfactant mesophase (Fig. 1), long-range organization is obtained at room temperature with surfac-

tant concentrations as low as 0.5% (by weight; as are all reactant concentrations herein), well within the range observed in biominerals. At these low concentrations, the cationic surfactants typically used in aqueous organic precursor solutions in mesophase syntheses [for example, cetyltrimethylammonium hydroxide (CTAOH), chloride, and bromide (CTAB)] form isotropic spherical or cylindrical micelles with no long-range order (13). For example, for 1% CTAB in water, in situ small-angle neutron scattering data reveal a broad scattering pattern characteristic of an isotropic micellar distribution (Fig. 2, inset). However, the addition of an aqueous silicate solution to the dilute CTAB solution leads to a significantly narrower scattering pattern (Fig. 2) that is consistent with an ordered, inorganic-organic hexagonal array. As will be shown, temperature- and composition-dependent silicate-surfactant mesophases can form, as evidenced by nuclear magnetic resonance (NMR) and freeze-fracture electron microscopy studies.

Deuterium NMR studies of ²H-labeled surfactant species in lyotropic liquid crystals (LLCs) have been widely used to probe aggregate geometries, molecular motions, and phase transitions (14). Anisotropic molecular motions lead to partial time-averaging of ²H quadrupole interactions, making the ²H NMR line shape sensitive to long-range organization of surfactant molecules. Figure 3A (15) shows the ²H NMR spectrum of 30% CTAB (deuterated at the α carbon position) in water at 35°C in the hexagonal LLC phase (16). The ²H quadrupole splitting, typically 126 kHz for an isotropic distribution of static C-²H units, is reduced to 11.5 kHz by various types of motions that the surfactant molecules undergo. In the lamellar LLC phase, the ab-

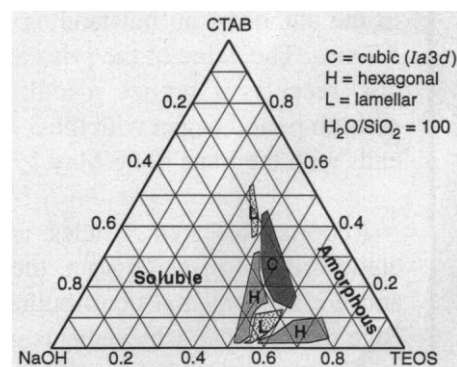


Fig. 1. Synthesis-space diagram of mesophase structures established by XRD measurements. Tetraethoxysilane (TEOS) was added in different concentrations to basic aqueous solutions of CTAB, such that each mixture overall had a H₂O/SiO₂ molar ratio of 100. The mixtures were stirred at room temperature for 1 hour before being heated at 100°C for 10 days.

A. Firouzi, L. M. Bull, T. Besier, S. A. Walker, J. A. Zasadzinski, B. F. Chmelka, Department of Chemical Engineering and Materials Research Laboratory, University of California, Santa Barbara, CA 93106, USA.

D. Kumar, P. Sieger, Q. Huo, D. Margolese, G. D. Stucky, Department of Chemistry, University of California, Santa Barbara, CA 93106, USA.

C. Glinka and J. Nicol, National Institute of Standards and Technology, Gaithersburg, MD 20899, USA.

*To whom correspondence should be addressed.

sense of rotational self-diffusion of the surfactant molecules about the cylindrical axis of the aggregate increases the quadrupole splitting by a factor of 2 (to ~ 23 kHz), consistent with experimental observations (14). A binary lamellar LLC phase consists of organic bilayers alternating with aqueous regions and is found for CTAB concentrations above $\sim 80\%$ (16).

The ordering observed for the hexagonal and lamellar phases in concentrated aqueous (aq) CTAB mixtures is in marked contrast to the isotropic configurations adopted by the surfactant molecules in dilute solutions, including those surfactant precursor solutions used in many mesophase syntheses (Fig. 1) (5–11). For example, the ^2H NMR spectrum (Fig. 3B) of a typical surfactant

precursor solution, containing 6.8% α -deuterated CTAB (aq), with all components except the silicate anions present, contains a single narrow peak. The isotropic ^2H NMR signal is consistent with isotropically mobile spherical micelles in dynamic equilibrium with monomeric surfactant molecules in solution (Fig. 4A) (16).

Long-range order in typical mesophase syntheses is achieved only after dilute isotropic aqueous silicate species are combined with a dilute isotropic surfactant solution. For example, after a 4.4% aqueous silicate solution at pH 13 is mixed with a spherical micellar 6.8% CTAB solution, a liquid crystalline mesophase precipitates rapidly. The spectrum in Fig. 3C contains two distinct contributions: (i) a narrow isotropic feature

and (ii) a scaled, axially symmetric Pake pattern that exhibits a quadrupole splitting of 12.5 kHz. Direct comparison to the ^2H quadrupole splittings associated with the hexagonal LLC of aqueous CTAB (Fig. 3A) reveals that the splitting of the Pake pattern (Fig. 3C) is due to the organization of surfactant molecules into cylindrical aggregates and is consistent with formation of a hexagonal silicate-surfactant mesophase. This mesophase can be considered as a silicateotropic liquid crystal (SLC) in which ordering is driven by interactions between the silicate and surfactant species.

Combining CTAB, water, multiply charged silicate anions, and organic additives, such as methanol and trimethylbenzene (TMB), produces phase behavior that is entirely different from that of aqueous CTAB, according to a more complicated multicomponent phase diagram, that must be determined. As will be shown, the morphology of the resulting mesophase precipitate depends strongly on controllable variables, such as mixture composition and temperature (6–9), and is established by various intra-aggregate and inter-aggregate interactions, most notably at the inorganic-organic interface.

The self-assembly of surfactants has been extensively studied (17), often with classical aggregation models, which balance forces at the interface constrained by geometric packing of individual surfactant molecules. Such general models must be extended to account explicitly for ion structure to predict the phase behavior of inorganic surfactant systems containing multiply charged ions with multiple coordination sites, such as aqueous silicate species at high pH, or gemini surfactants. Phase behavior is further complicated by distributions of such anionic species in solution, as are often present in recent syntheses of mesophase materials (5–11). The ^{29}Si solution-state NMR spectrum (18) in Fig. 5A, for example, shows peaks corresponding to an equilibrium mixture of various silicate species present in a typical mesophase precursor silicate solution at pH 13 before mixing with the aqueous CTAB solution. The dominant peak at -99.9 ppm is assigned to the eight identical Q^3 Si atoms in the double-four ring (D4R) (cubic octamer) silicate oligomer, $[\text{H}_n\text{Si}_8\text{O}_{20}]^{(8-n)-}$; Q^n represents the number of chemical bonds formed by a given Si atom to n other adjacent Si atoms through tetrahedrally bridging O atoms (19). To clarify the role of large multiply charged inorganic species (20) on the phase behavior of composite inorganic-organic assemblies, a precursor silicate solution containing specific silicate oligomers, such as double three-ring (D3R) or double four-ring (D4R) species, can be used to initiate

Fig. 2. Small-angle neutron scattering data for a dilute 1% CTAB- H_2O solution with and without dissolved silica. Filled circles (inset) outline the scattering pattern in the absence of dissolved silica, which reveals a single broad peak indicative of spherical micelles. The open circles indicate the scattering from the precipitated phase that forms when SiO_2 -NaOH, in a molar ratio of 1.5:1, is added to the solution. This phase exhibits a diffraction pattern characteristic of an ordered hexagonal array of rodlike aggregates, with a d spacing of 4.5 ± 0.2 nm.

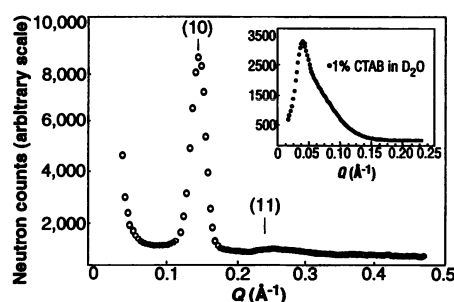
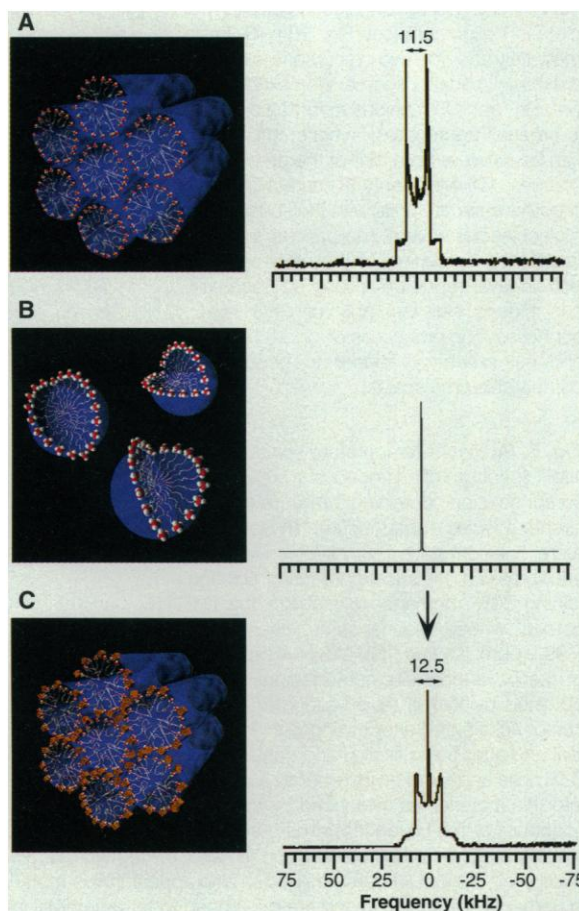


Fig. 3. The ^2H NMR spectra of α -deuterated CTAB in (A) a 30% aqueous solution at 35°C in a hexagonal LLC phase (16); (B) a 6.8% aqueous solution at 25°C , which reflects an isotropic surfactant environment consisting of spherical micelles (16); and (C) a hexagonal SLC phase at 25°C obtained immediately after the addition of a D4R silicate solution to the micellar surfactant solution whose spectrum is shown in (B). The resultant mixture had the following molar composition: 1.4 SiO_2 , 196 H_2O , 0.5 $(\text{TMA})_2\text{O}$, 0.25 $(\text{C}_{16}\text{TMA})_2\text{O}$, 18.8 CH_3OH .



mesophase assembly (Fig. 4A) (8). The conditions applied here, that is, Cab-o-sil as a silica source, trimethylammonium hydroxide (TMAOH), room temperature, and high pH, were chosen to favor the D4R oligomer (21). The addition of methanol further stabilizes D4R units (22), so that the ^{29}Si solution-state NMR spectrum of this system contains only the peak at -99.9 ppm (Fig. 5B).

The suitability of the D4R unit for forming silicate-surfactant mesophases is evident from the solid-state ^{29}Si magic-angle spinning (MAS) NMR spectrum (Fig. 5C) of a filtered and air-dried hexagonal mesophase material. A single narrow peak is observed at -99.9 ppm, with no other silicate oligomer species observed, consistent with preferential (but not necessarily exclusive) incorporation of intact D4R oligomers into the silicate-surfactant mesophase. Use of the stabilized precursor silicate solution containing the D4R oligomer (Fig. 5B) to form the air-dried hexagonal mesophase similarly yields a single peak at -99.9 ppm (Fig. 5D). Separate elemental analyses and x-ray diffraction (XRD) experiments of washed and unwashed samples confirm that this composite material is essentially an insoluble silicate-surfactant salt with a hexagonal mesostructure. Furthermore, the absence of a lower frequency Q^4 ^{29}Si NMR signal (upfield, to the right in the spectrum of Fig. 5, C and D) reveals that polymerization of silicate units is slowed to a negligible extent. Consequently, organization of the silicate-surfactant liquid crystal mesophase has occurred in the absence of interfacial silicate condensation, permitting detailed analysis of the mesophase self-assembly process alone, uncoupled from the kinetics of silica polymerization.

These results demonstrate ion exchange of nascent charge-compensating surfactant anions, Br^- and OH^- , by multiply charged D4R silicate anions after the precursor solutions have been combined (Fig. 4B). Several factors may account for the high mutual affinity between a surfactant head group and a D4R silicate oligomer, leading to the preferential exchange process observed. First, the D4R anions are highly ionized and are therefore multiply charged with correspondingly high anionic charge densities (20). Moreover, multidentate interaction of a head group with at least four O atoms on a D4R oligomer face is expected to enhance Coulombic attractions, thereby creating an especially stable configuration (as compared with coordination to a single corner $\equiv\text{Si}-\text{O}^-$ unit alone). Such multidentate coordination is facilitated by the complementary geometries of the D4R silicate unit and the surfactant head group (23). Thus, the D4R silicate species compete with and ion exchange for Br^- or OH^-

counterions and are preferred to the monomeric and smaller oligomeric silicate species (8). These results are consistent with dissociation constants for similar cationic surfactant systems, in which the effects of surface size and charge are well documented (25).

Multidentate complexation of multiply charged inorganic anions, such as the D4R silicate oligomers, to surfactant head groups has several important implications for the nucleation and growth of the inorganic-organic composite. For example, this multidentate bonding screens the intra-aggregate electrostatic head group repulsions among adjacent amphiphilic molecules, thereby reducing the average head group area, a_0 , available to a surfactant molecule and with it the local aggregate curvature. As a consequence, an aggregate can grow in size and possibly adopt a geometry with reduced curvature, so that during the ion-exchange process (Fig. 4B), inorganic-or-

ganic aggregates are formed with structures that will in general be entirely different from that of the precursor micelles. This behavior is analogous to the response of alkyltrimethylammonium bromide micellar solutions to the addition of electrolytes, which cause similar reductions in mean head group area and spherical-cylindrical micellar transitions (26–29). There appear to be numerous inorganic species besides silicate to which this applies, including tungstate, plumbate, and stibnate systems (9).

Strong binding of several head groups to double-ring silicate anions effectively creates multitailed silicate-surfactant units that collectively can further reduce the local curvature of the aggregate. For example, the surfactant-to-silicate molar ratio in the liquid crystal array studied here is determined by the degree of ionization of the silicate anions at the pH of the solution. Thermogravimetric analysis of the air-dried

Fig. 4. Schematic diagram of the cooperative organization of silicate-surfactant mesophases. (A) Organic and inorganic precursor solutions. Depending on the concentration of the surfactant, the initial organic precursor consists of spherical or cylindrical (or ellipsoidal) micelles that are in dynamic equilibrium with single surfactant molecules. The inorganic precursor solution at high pH contains predominantly multiply charged silicate anions [for example, D4R oligomers (see Fig. 5B)]. (B) Immediately after the two precursor solutions are mixed, silicate oligomers ion exchange with Br^- and OH^- anions to form inorganic-organic aggregates, whose structure can be different from that of the precursor micelles. (C) Multidentate interactions of oligomeric silicate units with the surfactant molecules has several implications. In particular, the screening of the electrostatic double-layer repulsion among aggregates can induce self-assembly of SLC mesophases. The processes of ion exchange and self-assembly appear to occur on comparable time scales.

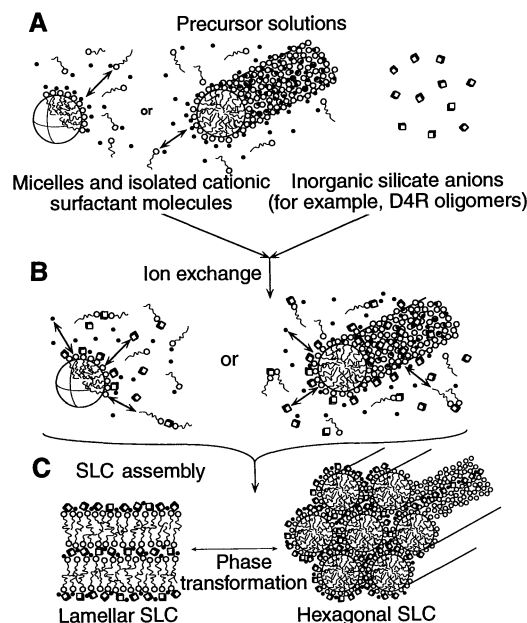
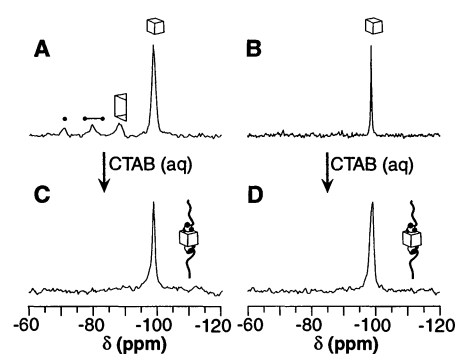


Fig. 5. (A) Room-temperature solution-state ^{29}Si NMR spectrum of an aqueous 10.0% silicate precursor solution containing a mixture of oligomeric silicate species at equilibrium. (B) Room-temperature solution-state ^{29}Si NMR spectrum of an equilibrated 4.4% silicate precursor solution containing 30% methanol to stabilize the D4R oligomer, whose resonance is clearly visible at -99.9 ppm. (C) The ^{29}Si MAS NMR spectrum (18) of the hexagonal silicate-surfactant mesophase obtained using the mixed-oligomer silicate precursor solution (A) after mixing with 12.8% CTAB (aq) and after being filtered and dried in air. Intact D4R units appear to be incorporated preferentially into this material, as evidenced by the single resonance peak at -99.9 ppm. (D) The ^{29}Si MAS NMR spectrum of the hexagonal silicate-surfactant mesophase (see Fig. 3C) obtained using the methanol-stabilized silicate precursor solution (B) after mixing with 12.8% CTAB (aq) and after being filtered and dried in air. Intact D4R silicate species also appear in this material. The chemical shifts (δ) are measured in parts per million (ppm) and are referenced to tetramethylsilane at 0 ppm.



salt shows that under the highly basic (pH 13) conditions used here, two to three cetyltrimethylammonium ions (CTA^+) bind on average to each D4R unit. A similar effect occurs in the conversion of micelles to bilayer vesicles in aqueous mixtures of single-tailed cationic and anionic surfactants (30). If complexation between surfactant molecules of opposite charge or between surfactant molecules and inorganic species produce "long"-lived physical complexes, then novel microstructures can be formed that would not exist in a solution containing the nascent surfactant species alone.

Interfacial charge screening due to strong silicate-surfactant multidentate bonding also

is expected to have a significant influence on the dynamic assembly of the ion-exchanged and modified aggregates. On the basis of the degree of ionization of CTAB in the isotropic organic precursor solution (26, 27), counteranions in the vicinity of the micelle surface contribute to a Debye-Hückel double layer that keeps the micelles separated. Addition of multiply charged double-ring silicate anions to this system results in rapid and strong binding of the silicate oligomers to the surfactant head groups, which reduces the double-layer thickness and thus, more effectively screens the electrostatic repulsions among aggregates and among isolated silicate-surfactant units. Above a certain threshold inorganic anion concentration, at-

tractive interfacial hydrophobic and van der Waals forces among aggregates will dominate interaggregate electrostatic repulsive forces. As a consequence, the system may self-assemble into a new ordered morphology (Fig. 4C) that will generally be different from the initial micelle structure in the precursor surfactant solutions (Fig. 4A). Similar precipitation phenomena have been observed for anionic phospholipid systems, where the addition of a concentrated divalent salt solution or the reduction of solution pH lowers the surface charge and can induce strong bilayer-bilayer adhesion, eventually leading to phase separation (31). Double four-ring silicate oligomers at an aggregate surface can furthermore satisfy residual charge-balancing requirements by binding to the surface of an adjacent aggregate, thereby stabilizing the assembly as the two aggregates coalesce.

Such changes reflect the approach of the silicate-surfactant mixture to a new thermodynamic equilibrium that, as for simple surfactant systems (for example, binary), balances electrostatic interactions at the aqueous inorganic-organic interface with interactions associated with the hydrophobic surfactant tails. For D4R silicate-surfactant systems, liquid crystalline mesophases separate from and coexist with more mobile micelle, and monomer species in solution. The precipitation of a mesophase produces a silicate-surfactant-rich phase in which the local concentration of surfactant is considerably higher than that in the initial precursor organic solution. Such SLC mesophases permit the establishment of long-range order similar to that found in conventional LLC phases, but at vastly lower overall bulk concentrations.

We have controlled the morphologies of unpolymerized silicate-surfactant mesophases (SLCs) within the constraints of a nominal inorganic-organic-water phase space by varying the relative concentrations of these species in the mixture. For example, addition of the stabilized D4R silicate precursor solution to a cylindrical micellar 12.8% aqueous CTAB (32) (Fig. 6A) produces rapidly and directly a silicate-surfactant mesophase. The 12.7-kHz ^2H quadrupole splitting in Fig. 6B reflects a hexagonal SLC, similar to that observed in Fig. 3C. The larger quadrupole splitting of the hexagonal SLC (12.7 kHz) with respect to that of a hexagonal LLC (11.5 kHz) indicates an increase in the order parameter and thus reduced mobility of the CTA^+ species in the presence of double-ring silicate polyanions (SLCs) compared to Br^- anions (LLCs) (33).

The role of the inorganic phase in modifying the organization of the organic array is further demonstrated by scattering and electron microscopy techniques, which

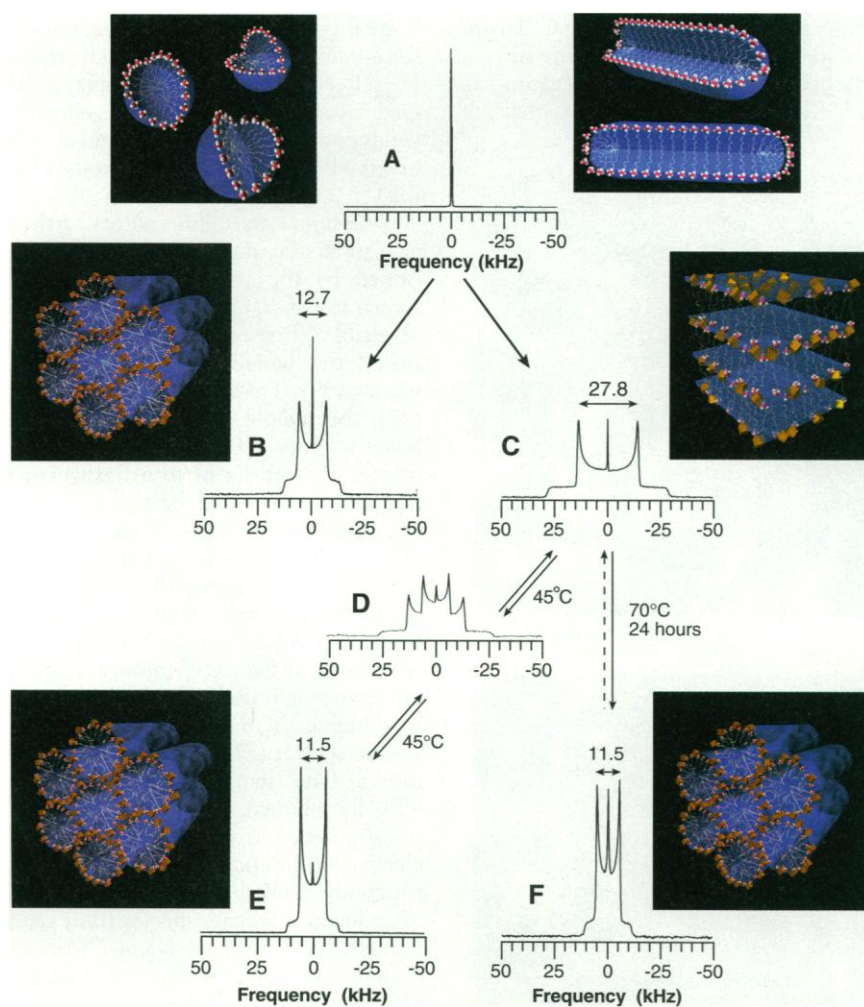


Fig. 6. ^2H NMR spectra of (A) an isotropic CTAB (aq) solution at 25°C representative of either cylindrical micelles (12.8% CTAB) or spherical micelles (6.8% CTAB). (B) A hexagonal SLC at 25°C (pure Q^3 silica) formed by the addition of the D4R silicate oligomer solution and TMB to an isotropic 12.8% CTAB (aq) solution (A); the resultant mixture had the following molar composition; 1.4 SiO_2 , 196 H_2O , 0.5 $(\text{TMA})_2\text{O}$, 0.5 $(\text{C}_{16}\text{TMA})_2\text{O}$, 18.8 CH_3OH , 1.2 TMB. (C) A lamellar SLC at 25°C (pure Q^3 silica) formed by the addition of the D4R silicate solution and TMB to an isotropic 6.8% CTAB (aq) solution (A), to form a mixture with the following molar composition; 1.4 SiO_2 , 196 H_2O , 0.5 $(\text{TMA})_2\text{O}$, 0.25 $(\text{C}_{16}\text{TMA})_2\text{O}$, 18.8 CH_3OH , 1.2 TMB. (D) An intermediate SLC mesophase formed from (C) after heating for 10 min at 45°C; a reversible first-order phase transformation occurs, as evidenced by superimposed ^2H powder patterns from coexisting lamellar and hexagonal phases (40). (E) A hexagonal SLC phase formed from (C) after equilibration for approximately 8 hours at 45°C (pure Q^3 silica remains). (F) A hexagonal SLC is formed irreversibly from the lamellar sample (C) after heating for 24 hours at 70°C ($\text{Q}^3/\text{Q}^4 \sim 1$).

probe order on longer length scales that are complementary to the molecular-level NMR studies. After filtering and air-drying the hexagonal silicate-surfactant mesophase from Fig. 6B, XRD data suggest the formation of a hexagonal mesostructure with a d spacing of 3.5 ± 0.2 nm, which corresponds to a center-to-center rod spacing of 4.0 nm (8, 34). Freeze-fracture transmission electron microscopy (TEM) (35) performed on the SLC precipitate yields images showing a region of well-aligned cylindrical aggregates (Fig. 7A) and a more common assembly of less-ordered rodlike aggregates (Fig. 7B) with a repeat distance of 7.0 ± 0.5 nm. This is consistent with a minimum-energy fracture plane (35) that has propagated along the staggered path 1 shown in Fig. 7A (left inset) and that can be shown, by simple geometry, to correspond to a center-to-center rod repeat distance of 4.0 ± 0.3 nm (36).

Reducing by 50% the surfactant-silicate

ratio of the reaction composition (to 6.8% CTAB), under conditions otherwise identical to those used in the mesophase synthesis of Fig. 6B, yields a lamellar SLC phase with a quadrupole splitting of 27.8 kHz (Fig. 6C) (37); XRD studies reveal an interlamellar d spacing of 3.9 ± 0.2 nm (7, 8). Deviation of the observed 27.8-kHz splitting in Fig. 6C from exactly twice the hexagonal-phase SLC splitting (25.4 kHz) is attributed to a larger order parameter associated with the lamellar SLC mesophase. Here, a lower surfactant concentration yields a lamellar, as opposed to a hexagonal, mesophase (8), a progression of phases that is opposite to the binary CTAB-water LLC system (16).

Freeze-fracture TEM images in Fig. 7, C and D, confirm the existence of a lamellar SLC mesophase for the material whose ^2H NMR spectrum is shown in Fig. 6C. Figure 7C shows a typical lamellar fracture surface with a bilayer spacing of 4.0 ± 0.3 nm, as

evidenced by the terraced discontinuities ranging from a few to tens of silicate-surfactant layers thick. What is unusual about this lamellar phase is the easily visible 4.0-nm wavelength undulations on the layer surfaces, which are likely closely associated with the hexagonal phase. The undulation wavelength is similar to the layer thickness and is probably determined by the length of two CTAB molecules. Apparently the undulations do not extend through the layers to form discrete cylindrical aggregates, as supported by the axially symmetric ^2H NMR spectra in Fig. 6, C through E. This suggests that the undulations in the layers have a fairly small amplitude or that the surfactant orientation does not vary significantly across the bilayer surface (8). A related ion-exchange reaction has recently been reported between sodium metatungstate and CTAOH, in which the salt, $(\text{C}_{19}\text{H}_{42}\text{N})_6(\text{H}_2\text{W}_{12}\text{O}_{40})$, adopts a puckered layer (monoclinic) arrangement that yields powder x-ray patterns similar to those observed for layered mesoporous silicates (38).

The liquid crystalline nature of the silicate-surfactant mesophases is clearly confirmed by the in situ ^2H NMR spectra shown in Fig. 6, C, D, and E, which show a reversible, first-order transformation between the lamellar and hexagonal SLC phases (39). Upon being heated to 45°C (40), the sample whose room-temperature lamellar-phase ^2H NMR spectrum is shown in Fig. 6C transforms to a hexagonal mesophase, as indicated by the reduction of the quadrupole splitting from 27.8 to 11.5 kHz (Fig. 6, D and E). Separate solid-state ^{29}Si MAS NMR spectra (not shown here) of the filtered and air-dried lamellar and hexagonal mesophases, whose ^2H spectra are shown in Fig. 6, C through E, contain only the single peak at -99.9 ppm, corresponding to the intact, unpolymerized D4R silicate species (7). Thus, for this system at intermediate temperatures (for example, 45°C for 8 hours), the thermodynamic SLC transformation is unaffected by slow polymerization kinetics of the silicate species, which are negligible on this time scale. For more reactive silicate species (for example, tetraethoxysilane; Figs. 1 and 2), however, or under the higher temperature conditions used in many mesophase syntheses (for example, 100°C) (5, 6, 9, 10), polymerization of the interfacial silicate species proceeds at a rate comparable to the silicate-surfactant self-assembly process, so that no equilibrium liquid crystal phases have been observed.

Following formation of a D4R silicate-surfactant SLC, interfacial silicate species can nevertheless be polymerized at higher temperatures or lower pH, forming an extended inorganic framework as the number of fully condensed Q^4 silicate species in-

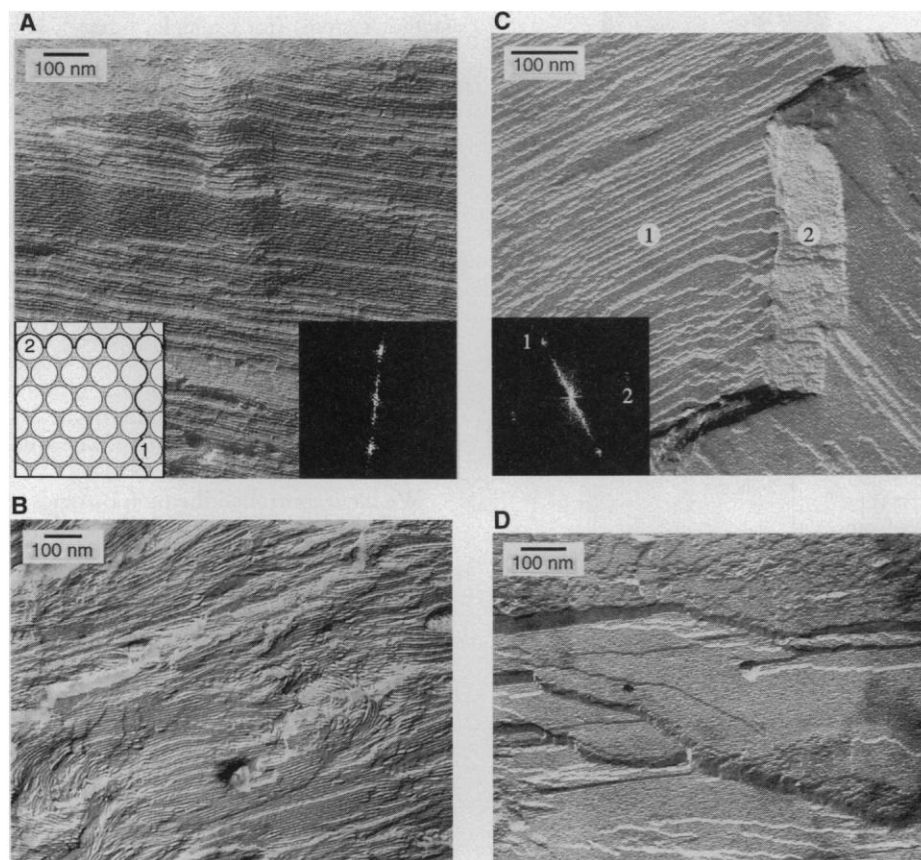


Fig. 7. Freeze-fracture transmission electron micrographs of platinum-carbon replicas of silicate-surfactant hexagonal and lamellar mesophases. **(A)** A region of well-aligned cylindrical aggregates in a hexagonal mesophase corresponding to Fig. 6B. The Fourier transform (FT) (right inset) shows periodicity (two bright spots above and below the center spot) corresponding to a rod center-to-center spacing of 7.0 ± 0.5 nm. The 7.0-nm spacing is consistent with a hexagonally close-packed array of aggregates with a center-to-center spacing of 4.0 ± 0.3 nm that has fractured along a staggered minimum-energy path (left inset, path 1). The energy cost for cleavage along path 2 is higher than for path 1. **(B)** A hexagonal mesophase (Fig. 6B) in which close packing of cylindrical aggregates displays reduced long-range order, a common feature of these samples. **(C)** A region of a lamellar mesophase corresponding to Fig. 6C. The FT (inset) shows two periodicities corresponding to (1) approximately 4.0 ± 0.3 -nm wavelength undulations on the lamellar surfaces and (2) approximately 4.0 ± 0.3 -nm aggregates. **(D)** A lamellar mesophase showing clearly visible undulations, whose directionality is preserved over many lamellar surfaces.

creases (7). For example, Fig. 6F shows the in situ ^2H NMR spectrum after heating for 24 hours at 70°C of the same material whose reversible liquid crystalline phase behavior is shown in Fig. 6, C through E. As observed for the silicate-surfactant system heated to 45°C (Fig. 6E), a similar transformation to a hexagonal mesophase occurs at the higher temperature, albeit much more rapidly (on the order of minutes). However, unlike the reversible low-temperature phase transition, after 24 hours at 70°C the structure does not return to the lamellar phase upon cooling to 25°C . Instead, the material retains a hexagonal mesostructure, with a d spacing of 3.9 ± 0.2 nm as established by separate XRD measurements (8), consistent with the formation of a polymerized silicate network that cannot reorganize back to a lamellar phase at 25°C . Solid-state ^{29}Si MAS NMR experiments (not shown here) confirm that the material treated at 70°C (Fig. 6F) contains a sizable fraction of polymerized Q^4 silica species ($\text{Q}^3/\text{Q}^4 \sim 1$) (7). Thus, silica polymerization can render SLC phase transitions irreversible. A closely related lamellar-hexagonal transformation was reported earlier in which the local aggregate curvature, and thus mesophase structure, was observed to depend on the extent of silica polymerization, according to charge-density matching requirements at the interface (6).

After polymerization of silicate species in the hexagonal mesophase sample associated with Fig. 6F at 70°C for 24 hours followed by calcination in O_2 at 600°C to remove the surfactant molecules, a mesoporous MCM-41 material is obtained (5) with hexagonally arranged channels and a BET surface area of ~ 900 m^2/g . The calcined material has an XRD pattern, ^{29}Si MAS NMR spectrum, and gas uptake properties that are characteristic of MCM-41 mesophase materials described by Kresge *et al.* (5). During polymerization, however, the silicate bonds of the D4R oligomers break or deform as the relatively disordered silicate network is extended. Nevertheless, on longer time scales, the system can anneal to produce a more ordered polymerized silicate structure, as evidenced by narrow Q^3 and Q^4 peaks in solid-state ^{29}Si MAS NMR spectra (7).

In summary, cooperative interactions among inorganic and organic species can lead to a variety of structures that would not be found in surfactant or inorganic systems alone. Electrostatic interactions, for example among aqueous silicate and surfactant species, cause the self-assembly of silicotropic liquid crystalline mesophases which possess long-range order governed by interfacial charge density and molecular packing considerations. By uncoupling self-assembly from inorganic polymerization, biomimetic and biomineralization synthesis strategies

may benefit from improved control of reaction processes. As a consequence, this provides new opportunities for understanding and utilizing biomimetic processes for structure-directing syntheses of novel composite materials.

REFERENCES AND NOTES

- S. Weiner, *Crit. Rev. Biochem.* **20**, 365 (1986); S. Weiner and W. Traub, *Philos. Trans. R. Soc. London Ser. B* **304**, 425 (1984); S. Mann *et al.*, *Science* **261**, 1286 (1993); S. Mann, *Nature* **365**, 499 (1993); B. R. Heywood and S. Mann, *Adv. Mater.* **6**, 9 (1994).
- S. Baral and P. Schoen, *Chem. Mater.* **5**, 145 (1993).
- D. D. Archibald and S. Mann, *Nature* **364**, 430 (1993).
- B. C. Bunker *et al.*, *Science* **264**, 48 (1994).
- C. T. Kresge *et al.*, *Nature* **359**, 710 (1992); J. S. Beck *et al.*, *J. Am. Chem. Soc.* **114**, 10834 (1992).
- A. Monnier *et al.*, *Science* **261**, 1299 (1993).
- D. Kumar *et al.*, in preparation.
- A. Firouzi *et al.*, in preparation.
- G. D. Stucky *et al.*, *Mol. Cryst. Liq. Cryst.* **240**, 187 (1994); Q. Huo *et al.*, *Chem. Mater.* **6**, 1176 (1994); Q. Huo *et al.*, *Nature* **368**, 317 (1994).
- C. Y. Chen, H. X. Li, M. E. Davis, *Microporous Mater.* **2**, 17 (1993); C. Y. Chen, S. L. Burkett, H. X. Li, M. E. Davis, *ibid.*, p. 27; M. E. Davis, C. Y. Chen, S. L. Burkett, R. F. Lobo, *Mater. Res. Soc. Symp. Proc.*, in press.
- V. Alfredsson *et al.*, *Chem. Commun.* **1994**, 921 (1994); A. Steel, S. W. Carr, M. W. Anderson, *ibid.*, p. 1571; M. Ogawa, *J. Am. Chem. Soc.* **116**, 7941 (1994).
- S. Mann, J. Webb, R. J. P. Williams, Eds., *Biomineralization: Chemical and Biochemical Perspectives* (VCH, Weinheim, 1989).
- F. Reiss-Husson and V. Luzzati, *J. Phys. Chem.* **68**, 3504 (1964); P. Ekwall, L. Mandell, P. Solyom, *J. Colloid Interface Sci.* **35**, 519 (1971); E. S. Blackmore and G. J. T. Tiddy, *Liq. Cryst.* **8**, 131 (1990).
- J. Seelig, *Quart. Rev. Biophys.* **10**, 353 (1977).
- We recorded the ^2H NMR spectra at 11.7 T on a Chemagnetics CMX-500 spectrometer operating at a frequency of 76.54 MHz and using a quadrupole echo pulse sequence. The ^2H $\pi/2$ pulse was typically 4 to 6 μs , with a 50- μs echo delay and a recycle delay of 0.25 s.
- X. Auvray *et al.*, *J. Phys. Chem.* **93**, 7458 (1989); T. Wörnheim and A. Jönsson, *J. Colloid Interface Sci.* **125**, 627 (1988).
- J. N. Israelachvili, D. J. Mitchell, B. W. Ninham, *J. Chem. Soc. Faraday Trans. 2* **72**, 1525 (1976); I. Szleifer *et al.*, *J. Chem. Phys.* **92**, 6800 (1990); for a review, see D. Langevin, *Annu. Rev. Phys. Chem.* **43**, 341 (1992).
- We recorded the ^{29}Si NMR spectra at 11.7 T on a Chemagnetics CMX-500 spectrometer operating at a frequency of 99.06 MHz and using proton decoupling during acquisition. The ^{29}Si $\pi/2$ pulse was typically 6 μs . For the solid samples, MAS at 5 kHz was used. The recycle delays for the liquid and solid samples were 30 s and 10 min, respectively.
- G. Engelhardt and D. Michel, *High Resolution Solid-State NMR of Silicates and Zeolites* (Wiley, New York, 1987), and references therein; G. Engelhardt and O. Rademacher, *J. Mol. Liq.* **27**, 125 (1984); Von D. Hoebbel, G. Garzó, G. Engelhardt, A. Vargha, *Z. Anorg. Allg. Chem.* **494**, 31 (1982).
- M. Wiebcke and D. Hoebbel, *J. Chem. Soc. Dalton Trans.* **16**, 2451 (1992).
- R. Harris and C. T. G. Knight, *J. Mol. Struct.* **78**, 273 (1982); E. J. J. Groenen *et al.*, *Zeolites* **6**, 403 (1986).
- W. M. Hendricks, A. T. Bell, C. J. Radke, *J. Phys. Chem.* **95**, 9519 (1991); C. T. G. Knight, *Zeolites* **9**, 448 (1989).
- The area of the D4R silicate oligomer face is ~ 0.093 nm^2 (20, 24), which matches closely the size of an $\text{N}(\text{CH}_3)_4^+$ ion (projected area ~ 0.094 nm^2). This apparently permits energetically favorable multidentate binding of a cationic surfactant head group to a D4R unit face with the anionic charge (and additional charge-balancing protons) distributed among the four corner O atoms.
- F. J. Fehr, T. H. Budzichowski, K. J. Weller, *J. Am. Chem. Soc.* **111**, 1288 (1989).
- D. F. Evans and D. D. Miller, in *Water Science Review*, F. Franks, Ed. (Cambridge Univ. Press, Cambridge, 1989), vol. 4, pp. 1-39.
- F. Quirion and L. J. Magid, *J. Phys. Chem.* **90**, 5435 (1986).
- C. Gamboa, H. Ríos, L. Sepúlveda, *ibid.* **93**, 5540 (1989).
- P. M. Lindemuth and G. L. Bertrand, *ibid.* **97**, 7769 (1993); S. Backlund, H. Hoiland, O. J. Kvammen, E. Ljosland, *Acta Chem. Scand. Ser. A* **36**, 698 (1982).
- S. Ozeki and S. Ikeda, *Bull. Chem. Soc. Jpn.* **54**, 552 (1981); S. Ikeda, *Colloid Polym. Sci.* **269**, 49 (1991).
- E. W. Kaler, A. K. Murthy, B. E. Rodriguez, J. A. N. Zasadzinski, *Science* **245**, 1371 (1989); A. K. Murthy, E. W. Kaler, J. A. Zasadzinski, *J. Colloid Interface Sci.* **145**, 598 (1991); E. W. Kaler, K. L. Herrington, A. K. Murthy, J. A. Zasadzinski, *J. Phys. Chem.* **96**, 6698 (1992); K. L. Herrington, E. W. Kaler, D. D. Miller, J. A. Zasadzinski, S. Chiruvolu, *ibid.* **97**, 13792 (1993).
- A. J. Verkleij *et al.*, *Biochim. Biophys. Acta* **339**, 432 (1974); K. Jacobson and D. Papahadjopoulos, *Biochemistry* **14**, 152 (1975); D. Papahadjopoulos *et al.*, *Biochim. Biophys. Acta* **394**, 483 (1975).
- In the absence of electrolytes (or organic solubilizers) the CTAB cylindrical micelles have been shown to be prolate ellipsoids with an aspect ratio of 2:1 (26).
- This enhancement of the order parameter is consistent with complexation of several surfactant molecules to each silicate oligomer, which is expected to reduce local motional averaging (8, 14).
- We acquired the XRD data on a Scintag PAD X using Cu K α radiation and a liquid nitrogen-cooled Ge solid-state detector. The data were collected from 1° to 30° (2θ) with a resolution of 0.02° and a count time of 2.4 s at each point.
- J. A. Zasadzinski and S. M. Bailey, *J. Electron Microsc. Tech.* **13**, 309 (1989).
- It is possible that the 7-nm periodicity reflects the closest spacing between less densely packed rods (Fig. 7A, left inset, path 2), however, this is not expected to be the energetically preferred fracture plane and has not been observed in XRD data or otherwise.
- Comparison of the spectra in Figs. 3C and 6C further demonstrates the significance of mixture composition. In the latter case, the incorporation of TMB, an expander molecule, into the hydrophobic region of the aggregate (28) reduces the local curvature, so that the lamellar mesophase is preferred.
- A. Stein *et al.*, in preparation.
- Superposition of the broader and narrower Pake patterns at an intermediate stage of the transition indicates that both lamellar and hexagonal SLC phases coexist, confirming that the thermodynamic transformation is first-order.
- At higher temperatures, TMB is expelled from the organic region of the aggregates (8). This effectively decreases the hydrophobic volume of the chains, which in turn enhances the local curvature of the surface, leading to formation of a hexagonal SLC phase. In addition, reequilibration of the D4R silicate species at higher temperatures to produce smaller oligomeric units, such as monomer, dimer, and D3R species, may contribute to the observed phase transition. The reverse processes occur during cooling to reproduce the lamellar SLC mesophase.
- We thank A. Oertl for assistance with deuteration of the surfactant and A. Schneider, S. Weigel, and L. Madsen for helpful discussions. This work was funded in part by the U.S. National Science Foundation (NSF) under the Materials Research Laboratory program (DMR-9123048) and under grant DMR-922527. B.F.C. acknowledges support from the NSF Young Investigator Program, the Camille and Henry Dreyfus Foundation, and the David and Lucile Packard Foundation. J.A.Z. and S.A.W. acknowledge support from Office of Naval Research grant N00014-90-J-1551, NSF grant CTS-9319447, and NIH grant GM 47334. This work was presented in part at the 10th International Zeolite Conference, July 1994, Garmisch-Partenkirchen, Germany.

5 July 1994; accepted 14 November 1994